Journal of the Korean Ceramic Society
Vol. 40, No. 5, pp. 401~404, 2003.

Electrochemical Properties of $LiNi_yMn_{2-y}O_4$ Prepared by the Solid-state Reaction

Myoung Youp Song,† Ik Hyun Kwon, and Mi Suk Shon

Division of Advanced Materials Engineering, The Research Center of Industrial Technology, Engineering Research Institute, Chonbuk National University, Jeonju 561-756, Korea

(Received September 4, 2002; Accepted March 24, 2003)

ABSTRACT

$LiNi_yMn_{2-y}O_4$ were synthesized by calcining a mixture of LiOH, MnO_2(CMD), and NiO at 400°C for 10 h and then calcining at 850°C for 48 h in air with intermediate grinding. The voltage vs. discharge capacity curves at a current density 300 $\mu A/cm^2$ between 3.5 V and 4.3 V showed two plateaus, but the plateaus became ambiguous as the y value increases. The sample with y=0.02 had the largest first discharge capacity, 118.1 mAh/g. As the value y increases from 0.02 up to 0.2, on the whole, the cycling performance became better. The $LiNi_{0.10}Mn_{1.90}O_4$ sample had a relatively large first discharge capacity 95.0 mAh/g and showed an excellent cycling performance. The samples with larger lattice parameter have, in general, larger discharge capacities. The reduction curves in the cyclic voltammograms for the y=0.05-0.20 samples exhibit three peak showing that the reduction may proceed in three stages in these samples. For the samples with relatively large discharge capacity, the lattice destruction induced by strain causes the capacity fading of $LiNi_yMn_{2-y}O_4$ with cycling.

Key words : $LiNi_yMn_{2-y}O_4$, Solid-state reaction, First discharge capacity, Cycling performance, Cyclic voltammograms, Capacity fading rate

1. Introduction

The transition metal oxides such as $LiCoO_2$,[1,2] $LiNiO_2$,[3,4] and $LiMn_2O_4$[5-9] have been investigated in order to apply them to a cathode material of lithium secondary battery. $LiCoO_2$ has high operating voltages and can be prepared easily. However, it contains an expensive element Co. $LiNiO_2$ has a large discharge capacity[10] and is relatively excellent from the view points of economics and environment. However, its preparation is very difficult as compared with $LiCoO_2$ and $LiMn_2O_4$. $LiMn_2O_4$ is very cheap and does not bring about environmental pollution, but its cycling performance is not good.

In our previous work,[11] the variation of the electrochemical properties of $LiMn_2O_4$ with the calcining temperature was investigated. The $LiMn_2O_4$ sample calcined at 850°C exhibited a relatively large discharge capacity and a quite good cycling performance.

In this work, in order to improve the cycling performance of $LiMn_2O_4$, a part of Mn in $LiMn_2O_4$ is replaced by Ni. $LiNi_yMn_{2-y}O_4$ samples were prepared by calcining at 850°C. Then their electrochemical properties were investigated.

2. Experimental

$LiMn_2O_4$ compound was synthesized by the solid-state reaction. A mixture of LiOH and MnO_2(CMD) with 1 : 2 molar ratio was calcined at 400°C for 10 h and then calcined twice at 850°C for 24 h in air with intermediate grinding. The samples were slowly cooled at a cooling rate of 1°C/min. After adding appropriate amounts of NiO to LiOH and MnO_2, $LiNi_yMn_{2-y}O_4$(y=0.02, 0.05, 0.10, 0.15, and 0.20) were also synthesized by the above same process. The phase identification of the prepared samples was carried out by X-Ray Diffraction (XRD, Rigaku III/A type) analysis using Cu Kα radiation. The morphology of the samples was observed using a Scanning Electron Microscope(SEM). To measure the electrochemical properties, the electrochemical cells consisted of the prepared sample as a positive electrode, Li metal as a negative electrode, and an electrolyte of 1 M $LiPF_6$ in a 2 : 1 (volume ratio) mixture of Ethylene Carbonate (EC) and Dimethly Carbonate (DMC). A Whatman glass-fiber was used as a seperator. The cells were assembled in an argon-filled dry box. To fabricate the positive electrode, 89 wt% active material, 10 wt% acetylene black, and 1 wt% Polytetrafluoroethylene (PTFE) binder were mixed in an agate mortar. By introducing Li metal, the Whatman glass-fiber, the positive electrode, and the electrolyte, the cell was assembled. All the electrochemical tests were performed at room temperature with a battery charge-discharge cycle tester (WonATec WBCS 3000) in a potential range from 3.5 V to 4.3 V. Fig. 1 summarizes the experimental procedure.

3. Results and Discussion

Fig. 2 shows XRD patterns of the $LiNi_yMn_{2-y}O_4$(y=0.00,

†Corresponding author : Myoung Youp Song
E-mail : songmy@moak.chonbuk.ac.kr
Tel : +82-63-270-2379 Fax : +82-63-270-2386

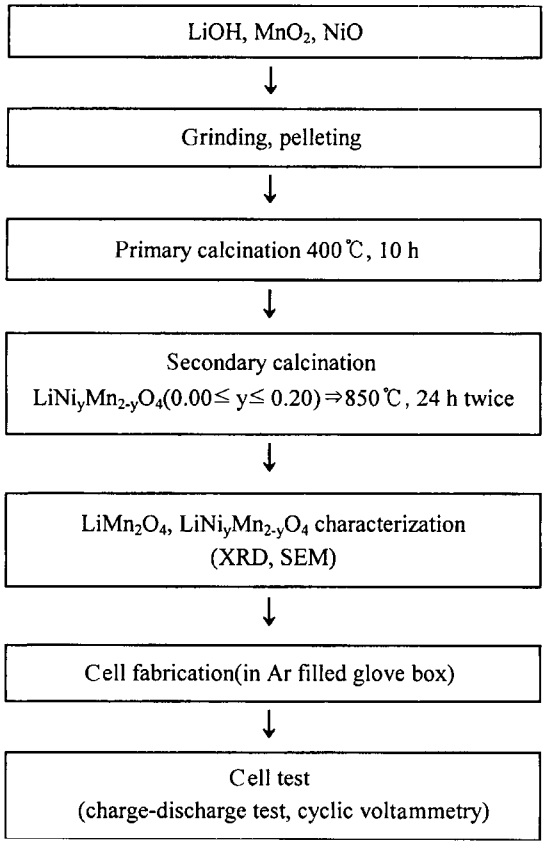

Fig. 1. Experimental procedure.

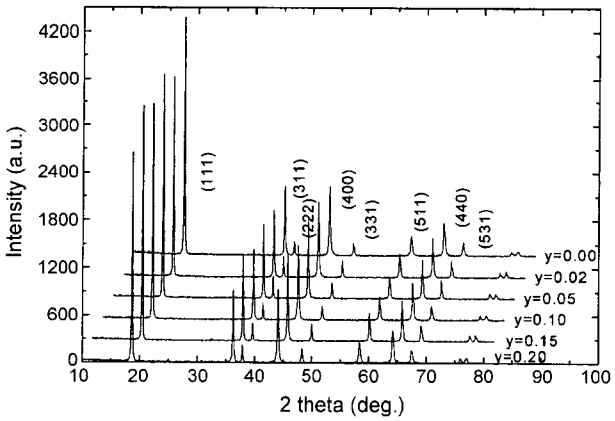

Fig. 2. XRD patterns of the $LiNi_yMn_{2-y}O_4$(y=0.00, 0.02, 0.05, 0.10, 0.15, and 0.20) samples calcined at 850°C.

Table 1. Lattice Parameters of the $LiNi_yMn_{2-y}O_4$ Samples Calcined at 850°C

Samples	Lattice parameter (Å)
$LiMn_2O_4$	8.214
$LiNi_{0.02}Mn_{1.98}O_4$	8.229
$LiNi_{0.05}Mn_{1.95}O_4$	8.228
$LiNi_{0.1}Mn_{1.9}O_4$	8.224
$LiNi_{0.15}Mn_{1.85}O_4$	8.210
$LiNi_{0.2}Mn_{1.8}O_4$	8.197

0.02, 0.05, 0.10, 0.15, and 0.20) samples calcined at 850°C for 24 h in air twice with intermediate grinding. All the samples exhibit similar patterns. They were identified as the cubic spinel phase having a space group Fd3m.

The lattice parameter of each sample was obtained by the least-squares method and is given in Table 1. It increases as the value of y increases from 0.00 to 0.02 and then it decreases as the value of y increases. The lattice parameters for y=0.00, 0.02 and 0.20 are 8.214, 8.229 and 8.197 Å, respectively.

Fig. 3 shows SEM micrographs of the $LiNi_yMn_{2-y}O_4$ samples. The sample for y=0.00 has relatively large particles with relatively homogeneous size. The samples from y=0.02 up to y=0.20 consist of very small particles and large particles. They have similar morphologies. It is considered that the addition of Ni makes the sample more brittle and the sample ground finer during intermediate grinding.

Fig. 4 shows the voltage vs. discharge capacity curves in a potential range from 3.5 to 4.3 V for the first cycle of the $LiNi_yMn_{2-y}O_4$ samples calcined at 850°C. The discharge capacity of the sample for y=0.02 is larger than those of the other samples. The curves for the y=0.02, 0.05 and 0.10 samples exhibit two plateaus which are quite distinct. Then the plateaus become ambiguous as the value of y increases further.

Fig. 5 shows the variations of discharge capacities for $LiNi_yMn_{2-y}O_4$ samples with the number of discharge cycle. The cells were cycled for 20 cycles at a current density 300 μA/cm^2 between 3.5 and 4.3 V. The first discharge capacity decreases in the order of the samples with y=0.02, 0.05, 0.00, 0.10, 0.15, and 0.20. The samples with y=0.00-0.10 have first discharge capacities 95.0-107.8 mAh/g. However, the samples with y=0.00 and 0.10 have better cycling performance than those with y=0.02 and 0.05. As the value y increases from 0.02 up to 0.20, on the whole, the cycling performance became better. At the 20th cycle, the sample with y=0.10 has the discharge capacity 95.5 mAh/g. This sample has the first discharge capacity (95.0 mAh/g). The discharge capacity of the y=0.10 sample remains almost constant during 20 discharge cycles. The sample with y=0.10 has a relatively large discharge capacity and an excellent cycling performance.

Fig. 6 shows cyclic voltammograms for the second charge-discharge cycles of the $LiNi_yMn_{2-y}O_4$ samples in the potential range from 3.5 to 4.3 V. The oxidation and reduction peaks are located around 4.07 V and 4.20 V. The reduction peaks for the y=0.00 and 0.02 samples are located at 3.92-3.95 V and 4.07-4.08 V. However, the reduction curves for the y=0.05, 0.10, 0.15, and 0.20 samples exhibit three peaks at 3.84-3.86 V, 3.93-3.96 V and 4.08-4.12 V. This shows that the reduction may proceed in three stages in these samples.

Fig. 7 gives the variations, with y in $LiNi_yMn_{2-y}O_4$, of lattice parameter, the first discharge capacity and capacity fading rate. The capacity fading rate, i.e. the decrease in the discharge capacity per no. of cycle, is obtained from the 3rd

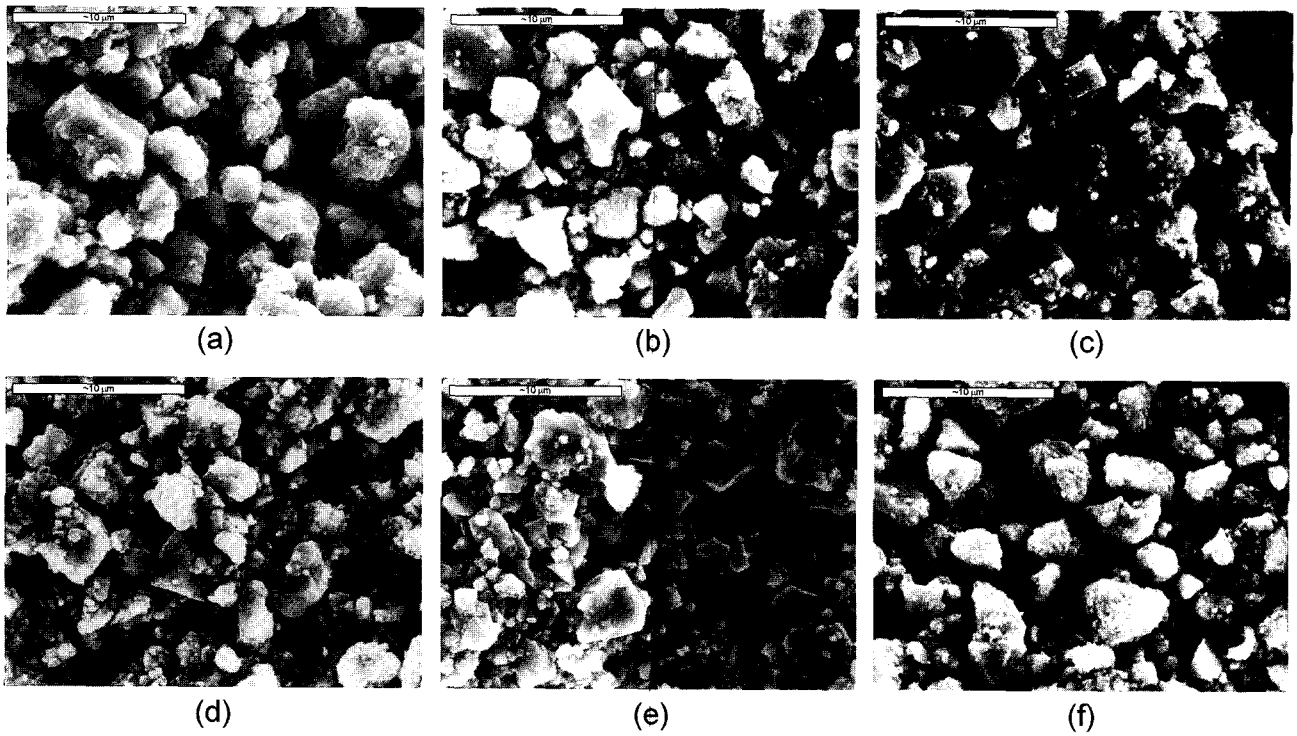

Fig. 3. SEM micrographs of the $LiNi_yMn_{2-y}O_4$ samples; (a) y=0.00, (b) y=0.02, (c) y=0.05, (d) y=0.10, (e) y=0.15, and (f) y=0.20.

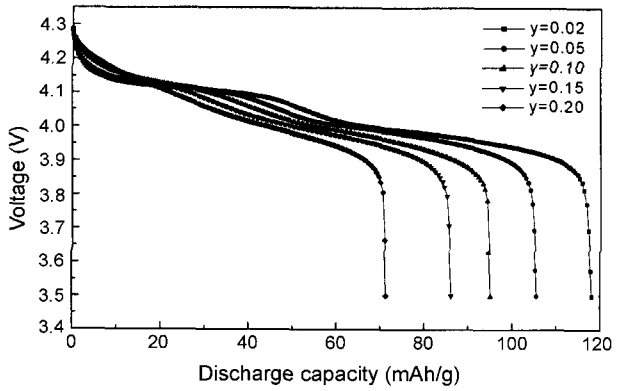

Fig. 4. Voltage vs. discharge capacity curves for the first cycle of the $LiNi_yMn_{2-y}O_4$ samples.

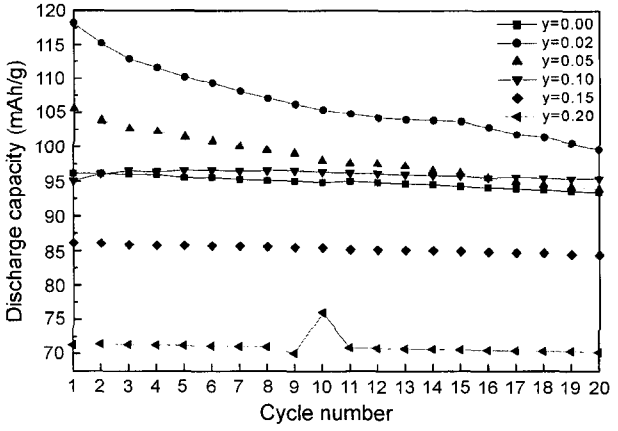

Fig. 5. Variations of the discharge capacities for the $LiNi_yMn_{2-y}O_4$ samples with the number of discharge cycle.

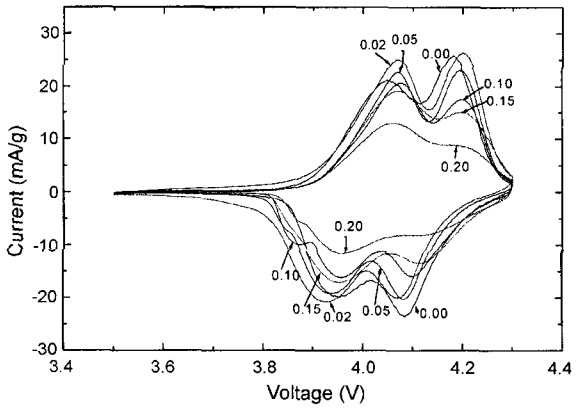

Fig. 6. Cyclic voltammograms for the second cycle of the $LiNi_yMn_{2-y}O_4$ samples.

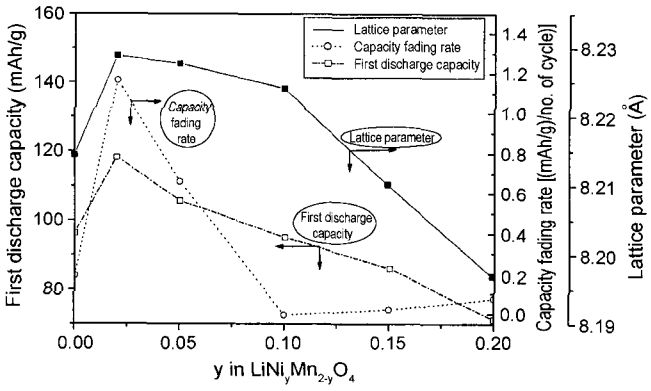

Fig. 7. Variations, with y in $LiNi_yMn_{2-y}O_4$, of lattice parameter, the first discharge capacity and capacity fading rate.

to the 7th cycle. The lattice parameter and the first discharge capacity increase from y=0.00 to y=0.02 and then they decrease from y=0.02 to y=0.20. This shows that the sample with a larger lattice parameter has the larger first discharge capacity, suggesting that the spinel structure with the larger lattice parameter intercalates and deintercalates the more Li ions. The capacity fading rate increases from y=0.00 to y=0.02 and they decrease from y=0.02 to y=0.10 and finally they increase in some degree. The larger first discharge capacity is related to the wider range of the value of x in $Li_xMn_2O_4$. The larger range of the value of x will cause the larger expansion and contraction of the spinel phase $LiMn_2O_4$ due to the intercalation and deintercalation. This will make the unit cell strained and distorted. With cycling, the interstitial sites and thus the spinel structure will be destroyed. This decreases the fraction of the spinel phase, leading to the capacity fading of $LiMn_2O_4$ with cycling. For the samples with the smaller discharge capacity, the expansion and contraction due to intercalation and deintercalation can be within the limit of elasticity of $LiNi_yMn_{2-y}O_4$, and thus the lattice destruction will not occur. The discharge capacity can remain constant (i.e., the capacity fading rate is almost zero) accordingly.

4. Conclusions

XRD patterns of all the synthesized samples exhibited the cubic spinel phase with a space group Fd3m. The electrochemical cells were charged and discharged for 20 cycles at a current density 300 $\mu A/cm^2$ between 3.5 V and 4.3 V. The voltage vs. discharge capacity curves for the samples showed two plateaus, but the plateaus became ambiguous as the y value increases. The sample with y=0.02 had the largest first discharge capacity 118.1 mAh/g. As the value y increases from 0.02 up to 0.2, on the whole, the cycling performance became better. The $LiNi_{0.10}Mn_{1.90}O_4$ sample had a relatively large first discharge capacity 95.0 mAh/g and a discharge capacity 95.5 mAh/g at the 20th cycle, showing that it has a excellent cycling performance. The samples with larger lattice parameter have, in general, larger discharge capacities. The cyclic voltammograms for the second cycle of the $LiNi_yMn_{2-y}O_4$ samples showed the oxidation and peaks around 4.07 V and 4.20 V. The reduction peaks for the y=0.00 and 0.02 samples are located at 3.92–3.95 V and 4.07–4.08 V. However, the reduction curves for the y=0.05–0.20 samples exhibit three peaks at 3.84–3.86 V, 3.93–3.96 V and 4.08–4.12 V. This shows that the reduction may proceed in three stages in these samples. For the samples with relatively large discharge capacity, the lattice destruction induced by strain causes the capacity fading of $LiNi_yMn_{2-y}O_4$ with cycling.

Acknowledgements

This work was supported by The Research Center of Industrial Technology, Engineering Research Institute, at Chonbuk National University.

REFERENCES

1. R. Alcantara, P. Lavela, J. L. Tirado, R. Stoyanova, and E. Zhecheva, "Structure and Electrochemical Properties of Boron-doped $LiCoO_2$," *J. Solid State Chem.*, **134** 265-73 (1997).
2. Z. S. Peng, C. R. Wan, and C. Y. Jiang, "Synthesis by Sol-gel Process and Characterization of $LiCoO_2$ Cathode Materials," *J. Power Sources*, **72** 215-20 (1998).
3. J. M. Tarascon, E. Wang, F. K. Shokoohi, W. R. McKinnon, and S. Colson, "The Spinel Phase of $LiMn_2O_4$ as a Cathode in Secondary Lithium Cells," *J. Electrochem. Soc.*, **138** 2859-64 (1991).
4. M. Y. Song and R. Lee, "Synthesis by Sol-gel Method and Electrochemical Properties of $LiNiO_2$ Cathode Materials for Lithium Secondary Battery," *J. Power Sources*, **4863** 1-7 (2002).
5. J. R. Dahn, U. von Sacken, and C. A. Michal, "Structure and Electrochemistry of $Li_{1+y}NiO_2$ and a New Li_2NiO_2 Phase with the $Ni(OH)_2$ Structure," *Solid State Ionics*, **44** 87 (1990).
6. J. R. Dahn, U. von Sacken, M. W. Juzkow, and H. Al-Janaby, "Rechargeable $LiNiO_2$/Carbon Cells," *J. Electrochem. Soc.*, **138** 2207-12 (1991).
7. M. Y. Song and D. S. Ahn, "On the Capacity Deterioration of Spinel Phase $LiMn_2O_4$ with Cycling around 4 V," *Solid State Ionics*, **112** 21-2 (1998).
8. M. Y. Song, D. S. Ahn, and H. R. Park, "Capacity Fading of Spinel Phase $LiMn_2O_4$ with Cycling," *J. Power Sources*, **83** 57-60 (1999).
9. Y. Xia and M. Yoshio, "An Investigation of Lithium Ion Insertion into Spinel Structure Li-Mn-O Compounds," *J. Electrochem. Soc.*, **143** 825-34 (1996).
10. Y. Nishida, K. Nakane and T. Stoh, "Synthesis and Properties of Gallium-doped $LiNiO_2$ as the Cathode Material for Lithium Secondary Batteries," *J. Power Sources*, **68** 561-64 (1997).
11. M. Y. Song and M. S. Shon, "Variations of the Electrochemical Properties of $LiMn_2O_4$ with the Calcining Temperature," *J. Kor. Ceram. Soc.*, **39** [6] 523-27 (2002).